Mutational, Kinetic, and NMR Studies of the Mechanism of *E. coli* GDP-Mannose Mannosyl Hydrolase, an Unusual Nudix Enzyme†

Patricia M. Legler, Michael A. Massiah, and Albert S. Mildvan*

Department of Biological Chemistry, The Johns Hopkins School of Medicine, 725 North Wolfe Street, Baltimore, Maryland 21205-2185

Received May 15, 2002; Revised Manuscript Received June 27, 2002

ABSTRACT: GDP-mannose mannosyl hydrolase (GDPMH) is an unusual Nudix family member, which catalyzes the hydrolysis of GDP-α-D-mannose to GDP and the β-sugar by nucleophilic substitution at carbon rather than at phosphorus (Legler, P. M., Massiah, M. A., Bessman, M. J., and Mildvan, A. S. (2000) *Biochemistry 39*, 8603−8608). Using the structure and mechanism of MutT, the prototypical Nudix enzyme as a guide, we detected six catalytic residues of GDPMH, three of which were unique to GDPMH, by the kinetic and structural effects of site-specific mutations. Glu-70 (corresponding to Glu-57 in MutT) provides a ligand to the essential divalent cation on the basis of the effects of the E70Q mutation which decreased k_{cat} $10^{2.2}$-fold, increased the dissociation constant of Mn^{2+} from the ternary E−Mn^{2+}−GDP complex 3-fold, increased the K_m^{Mg2+} 20-fold, and decreased the paramagnetic effect of Mn^{2+} on $1/T_1$ of water protons, indicating a change in the coordination sphere of Mn^{2+}. In the E70Q mutant, Gln-70 was shown to be very near the active site metal ion by large paramagnetic effects of Mn^{2+} on its side chain $-NH_2$ group. With wild-type GDPMH, the effect of pH on log($k_{cat}/K_m^{GDPmann}$) at 37 °C showed an ascending limb of unit slope, followed by a plateau yielding a pK_a of 6.4, which increased to 6.7 ± 0.1 in the pH dependence of log(k_{cat}). The general base catalyst was identified as a neutral His residue by the $\Delta H^{ionization}$ = 7.0 ± 0.7 kcal/mol, by the increase in pK_a with ionic strength, and by mutation of each of the four histidine residues of GDPMH to Gln. Only the H124Q mutant showed the loss of the ascending limb in the pH versus log(k_{cat}) rate profile, which was replaced by a weak dependence of rate on hydroxide concentration, as well as an overall $10^{3.4}$-fold decrease in k_{cat}, indicating His-124 to be the general base, unlike MutT, which uses Glu-53 in this role. The H88Q mutant showed a $10^{2.3}$-fold decrease in k_{cat}, a 4.4-fold increase in $K_m^{GDPmann}$, and no change in the pH versus log(k_{cat}) rate profile, indicating an important but unidentified role of His-88 in catalysis. One and two-dimensional NMR studies permitted the sequence specific assignments of the imidazole Hδ2C, Hε1C, Nδ1, and Nε2 resonances of the four histidines and defined their protonation states. The pK_a of His-124 (6.94 ± 0.04) in the presence of saturating Mg^{2+} was comparable to the kinetically determined pK_a at the same temperature (6.40 ± 0.20). The other three histidines were neutral Nε2H tautomers with pK_a values below 5.5. Arg-52 and Arg-65 were identified as catalytic residues which interact electrostatically with the GDP leaving group by mutating these residues to Gln and Lys. The R52Q mutant decreased k_{cat} 309-fold and increased $K_m^{GDPmann}$ 40.6-fold, while the R52K mutant decreased k_{cat} by only 12-fold and increased $K_m^{GDPmann}$ 81-fold. The partial rescue of k_{cat}, but not of $K_m^{GDPmann}$ in the R52K mutant, suggests that Arg-52 is a bifunctional hydrogen bond donor to the GDP leaving group in the ground state and a monofunctional hydrogen bond donor in the transition state. Opposite behavior was found with the Arg-65 mutants, suggesting this residue to be a monofunctional hydrogen bond donor to the GDP leaving group in the ground state and a bifunctional hydrogen bond donor in the transition state. From these observations, a mechanism for GDPMH is proposed involving general base catalysis and electrostatic stabilization of the leaving group.

The Nudix family of hydrolytic enzymes is defined by the presence of the Nudix box sequence (Figure 1) (*1*). Approximately 800 proteins in more than 80 different species contain such a sequence. Nudix hydrolases have been shown to catalyze the hydrolysis of nucleoside diphosphate derivatives by nucleophilic substitution at phosphorus on the basis of their reaction products, or in some cases, by $H_2{}^{18}O$ incorporation (*2*−*4*). Homodimeric GDP-mannose mannosyl hydrolase (GDPMH)[1] from *Escherichia coli* is the most unique member of the Nudix family in that it differs from other Nudix enzymes in five ways. First, it catalyzes the attack by water[2] at the C1′ carbon of the sugar rather than at the β-phosphorus, yielding GDP and the β-sugar (*5*):

$$\text{GDP-}\alpha\text{-D-mannose} + H_2O \rightarrow \text{GDP} + \beta\text{-D-mannose} + H^+ \quad (1)$$

$$\text{GDP-}\alpha\text{-D-glucose} + H_2O \rightarrow \text{GDP} + \beta\text{-D-glucose} + H^+ \quad (2)$$

† This research was supported by the National Institutes of Health Grants DK28616 (to A.S.M.) P.M.L. was supported by a National Science Foundation Pre-doctoral Fellowship.

* To whom correspondence should be addressed. Phone: 410-955-2038. E-mail: mildvan@welchlink.welch.jhu.edu. Fax: 410-955-5759.

10.1021/bi020362e CCC: $22.00
Published on Web 08/07/2002

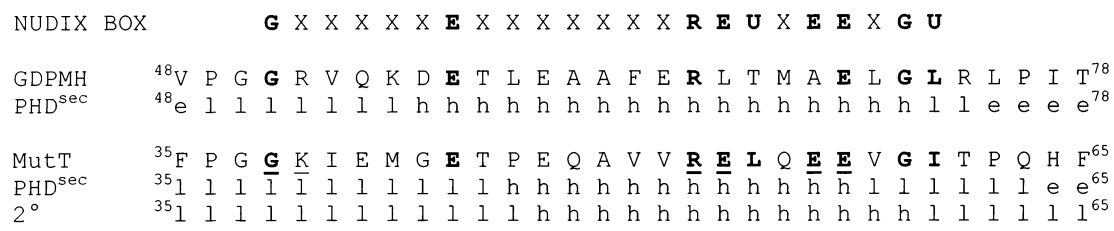

FIGURE 1: Nudix Box sequences of the GDP-mannose mannosyl hydrolase and the MutT NTP pyrophosphohydrolase. Beneath each sequence are the PHD secondary structure predictions (33) and the actual secondary structure of the MutT enzyme (11). The bold residues are conserved, and the underlined residues are in the active site of MutT. Note that residue N+13 of the Nudix Box of GDPMH corresponds to residue N of MutT.

Second, the Nudix box of GDPMH contains the sequence ^{64}ER^{65} instead of ^{52}RE^{53}, as found in the MutT pyrophosphohydrolase, the prototypical Nudix enzyme, and in other Nudix enzymes.[3] In MutT, Glu-53 is believed to function as a reversible metal ligand and as the general base, which is positioned by Arg-52 to deprotonate the attacking H_2O (*6*). The shifting of Glu to a position preceding the conserved Arg in GDPMH removes the homologous general base, suggesting that GDPMH uses a different residue for this purpose or that it may not require a general base. Third, the GDPMH Nudix box lacks a conserved glutamate residue, corresponding to Glu-56 of MutT, where it was identified as a metal ligand (*6*, *7*). Fourth, GDPMH is comparably activated by either Mn^{2+} or Mg^{2+} and shows similar affinities for both metal ions (*8*). Other enzymes, including the Nudix enzymes MutT and Ap_4AP, show at least 1 order of magnitude greater affinity for Mn^{2+} than for Mg^{2+} (*9*, *10*). Fifth, GDPMH was previously shown to require only one metal ion in its active site (*8*), unlike MutT, which requires two (*9*), or Ap_4A pyrophosphohydrolase (Ap_4AP), which requires three (*10*). By a pulsed EPR method, electron spin−echo envelope modulation (ESEEM) spectroscopy, the tightly bound active site metal ion of GDPMH was shown to form an inner sphere enzyme−Mn^{2+}−GDP metal bridge complex (*8*).

While the solution structures of MutT (*11*) and Ap_4AP (*12*) and the X-ray structure of ADP-ribose hydrolase (*13*) have been determined, the three-dimensional structure of GDPMH is unknown. Two and three-dimensional heteronuclear NMR studies indicated multiple conformations of this homodimer, precluding complete resonance assignments.[4] While crystals of GDPMH which diffracted to 2.0 Å were obtained, they showed a high degree of merohedral twinning under many conditions, precluding an X-ray structure.[5] Hence, alignment of the primary structure of GDPMH with that of the MutT enzyme (Figure 1) has been used as a guide for mutagenesis studies to determine the catalytic residues of GDPMH. With the exception of residues corresponding to Glu-53 and Glu-56 in MutT, all other residues in the GDPMH Nudix box are conserved.[6] Therefore, the functions of both conserved and nonconserved residues in the GDPMH Nudix box were studied by mutagenesis. Six residues were found to contribute significantly to catalysis, three of which were unique to GDPMH.

EXPERIMENTAL PROCEDURES

Materials. The nucleotides GDP and GDP-α-D-mannose were purchased from Sigma. The nucleotides and buffers were passed over Chelex-100 resin to remove trace metal contaminants. SigmaUltra ammonium sulfate, MES buffer, and malachite green were also purchased from Sigma (St. Louis, MO). HEPES and MOPS buffers were purchased from Fisher Scientific (Fair Lawn, NJ). Ultrapure (99.995%) $MnCl_2$ was purchased from Johnson Matthey Chemicals Limited (London, England). Ultrapure (99.995%) $MgCl_2$ hexahydrate was purchased from Aldrich Chemical Co. (Milwaukee, WI). Ultrafiltration concentrators were purchased from Vivascience (polyethersulfone membrane, 10 000 MWCO, Gloucestershire, UK). Ecolite(+) scintillation cocktail was from ICN Biomedicals, Inc. (Costa Mesa, CA). *E. coli* strain DH5α was purchased from Gibco BRL (Grand Island, NY). *E. coli* strain BL-21(DE3) Epicurian Coli was purchase from Stratagene (LaJolla, CA). Restriction enzymes were purchased from New England Biolabs (Beverly, MA) and Gibco BRL. Plasmid DNA purification kits were purchased from Qiagen (Valencia, CA). ^{15}N-labeled ammonium chloride was purchased from Isotec (Miamisburg, OH). ^{3}H-labeled GDP-mannose was purchased from New England Nuclear Life Science Products (Boston, MA); the nonexchangeable tritium was present on the C2′ of the mannose moiety. The tritiated GDP-mannose was supplied in 70% ethanol and was lyophilized before use.

General Methods. E. coli strain DH-5α was used for subcloning. The construction of the wild-type petGDPMH

[1] Abbreviations: AEBSF, 4-(2-aminoethyl)benzenesulfonyl fluoride; Ap_4AP, diadenosine pyrophosphatase; BCA, bicinchoninic acid; EDTA, (ethylenedinitrilo)tetraacetic acid; EPR, electron paramagnetic resonance; ESEEM, electron spin−echo envelope modulation; FID, free induction decay; GDP, guanosine diphosphate; GDPMH, GDP-mannose mannosyl hydrolase; HEPES, 4-(2-Hydroxyethyl)-1-piperazineethanesulfonic acid; HSQC, heteronuclear single-quantum coherence; LB/Amp, Luria-Bertani medium containing ampicillin; MES, 2-[N-morpholino]ethanesulfonic acid; MutT, MutT NTP pyrophosphohydrolase; MWCO, molecular weight cutoff; NMR, nuclear magnetic resonance; 3D-NOESY, three-dimensional nuclear overhauser effect spectroscopy; Nudix, nucleoside diphosphate-X; PCR, polymerase chain reaction; PRR, proton relaxation rate; TPPI, time-proportional phase increment.

[2] No evidence for disaccharide formation was observed by thin-layer chromatography after adding 30 mM D-glucose, D-fucose, L-fucose, L-rhamnose, *N*-acetyl-D-glucosamine, D-glucosamine, or D-mannose to the reaction mixture containing 30 mM GDP-mannose, 40 mM glycine at pH 9.3, and 10 mM $MgCl_2$ (incubated for 165 min at 37 °C). Hence, water is the only known nucleophile for the glycosyl transfer reaction of GDPMH. Legler, P. M. (2002) unpublished observations.

[3] Changing the sequence from ^{64}ER^{65} in wild-type GDPMH to ^{64}RE^{65} by a double mutation resulted in a 10^3-fold loss of GDP-mannose hydrolase activity and the appearance of no detectable MutT-like activity. Legler, P. M. (2001) unpublished observations.

[4] Legler, P. M., and Massiah, M. A. (1998) unpublished observations.

[5] Legler, P. M., and Gabelli, , S. B. (2002) unpublished observations.

[6] Residue N+13 of the Nudix box of GDPMH corresponds to residue N of MutT.

plasmid and purification of the GDPMH enzyme were described previously (*14*). *E. coli* strain BL-21(DE3), used for protein expression, was grown in MOPS media (*15*) with either unlabeled or ^{15}N-labeled ammonium chloride in the presence of 100 μg/mL ampicillin at 37 °C. The R65Q, R65K, H102Q, and H142Q mutants expressed insoluble protein when induced at 37 °C for 2 h and soluble protein when induced at 16 °C for 20 h. The R52K mutant was expressed at 22 °C for 20 h to obtain soluble protein. An additional G-25 Sephadex (25 cm × 1 cm) desalting column equilibrated with 80 mM Na^+ HEPES pH 7.5 was used at the end of the purification to remove EDTA present in prior purification steps.

Lower activity was noted for two mutants, E70Q and H88Q, after the DEAE Sepharose column, most likely due to protein instability in the low ionic strength DEAE Sepharose buffer. The highest measured specific activities after the G-50 Sephadex column alone were reported for these two mutants. After the G-50 and G-25 Sephadex columns, the E70Q and H88Q mutants were judged to be at least 90% pure on the basis of Coomassie-stained gels. After the G-50 Sephadex, DEAE Sepharose, and G-25 Sephadex columns, all other enzymes were judged to be at least 95% pure on the basis of Coomassie-stained gels. All of the mutants eluted as ~36 kDa dimers from a calibrated G-50 Sephadex column like the wild-type enzyme. Protein concentrations were measured using the BCA Assay Kit as directed or by the method of Von Hippel et al. (*16*); the two methods differed by 3%.

Preparation of GDPMH Mutants. The modified megaprimer method (*17*) as described by Barik (*18*) was used to prepare the GDPMH mutants. The wild-type GDPMH plasmid was used as a template for the PCR reaction to generate the megaprimer. The 3′ primer which contained the appropriate mispair (underlined) in the codon of the amino acid to be mutated (Table 1) and a 5′ primer containing an NdeI restriction site (underlined) (*14*) were used (CG CGC GCG CAT ATG ATG TTT TTA CGT CAG GAA GAC) in the synthesis of the megaprimer. The megaprimer was purified by gel extraction (2% agarose gel) to separate it from the wild-type template plasmid DNA using the Qiagen Gel Extraction Kit as recommended. The megaprimer was then used in a second PCR reaction with the 3′ primer which contained a BamHI restriction site (underlined) (*14*) (CG CGC GGA TCC TCA TAA TCC GGG TAC TCC GGT ACG) to generate the full-length mutant insert with NdeI (5′ end) and BamHI (3′ end) cleavage sites. The full-length insert was cut with BamHI and NdeI and ligated into a pet11b plasmid which had been cut with the same restriction enzymes and treated with alkaline phosphatase. The PCR protocol consisted of a hot start at 94 °C for 5 min and 35 cycles; one cycle consisted of a 94 °C denaturation for 40 s, 58 °C annealing for 30 s, and elongation at 72 °C for 30 s. After 35 cycles, the reactions were incubated at 72 °C for 10 min and kept at 4 °C. The ligated plasmid was subcloned into DH5α *E. coli* cells. The plasmid DNA was then purified using the Qiagen miniprep kit and then cloned into BL-21(DE3) *E.coli* cells for protein expression. All plasmids containing inserts were isolated and sequenced to verify the mutation and the otherwise unaltered DNA sequence.

GDPMH Assay. The assay used to measure the hydrolysis of GDP-mannose was previously described (*5*, *14*). Briefly, the production of GDP during the course of the reaction was followed by measuring the concentration of phosphate produced upon treatment of the GDP product with calf intestinal alkaline phosphatase in a coupled enzyme assay. Alkaline phosphatase does not affect the GDP-mannose substrate. All mutants were assayed at 37 °C, pH 9.3, for 15−20 min using 1−2 mU of enzyme. Other components present were 80 mM Glycine buffer pH 9.3, 20 mM $MgCl_2$, and 1 U of calf intestinal alkaline phosphatase. The low activity of the H102Q mutant was measured using a similar assay with a second dye, malachite green oxalate, to enhance the detection of molybdate phosphate (*19*). The K_m and V_{max} values were extrapolated from double reciprocal plots of the velocity versus substrate concentrations.

Table 1: Primers Used for the Construction of GDPMH Mutants[a]

mutation	primer sequence
	HhaI
E70Q	CAAACGCAGCCCCAG**TTGCGC**CATCGTCAGCCG
	PstI
E60Q	CCGCTCAAATGCGGC**CTGCAG**CGTTTCGTCTTT
	AlwNI
E64Q	CGCCATCGT**CAG**CCG**CTG**AAATGCGGCTTCCAG
	none
A69E	CAGCCCCAGTTCCTCCATCGTCAGCCGCTC
	none
H88Q	GTTATCGTCATAAAACTGTTGCCAGACACCGTA
	none
H102Q	ACCGAGCACCACATACTGAGTGGTGAAATCCGT
	none
H124Q	CCAGCGGTAATCGTCCTGTTGCTCATCCGGCAG
	EcoRI
H142Q	AAAATAGGCGCGG**GAATTC**GCCTGAACATTATC
	(HhaI)
R52Q	TTCGTCTTTCTGCA**CCTGC**CCCTCCCGGCACAAA
	(HhaI)
R52K	TTCGTCTTTCTGCA**CTTT**CCCTCCCGGCACAAA
	AluI
R65Q	TTCCGCCATCGTC**AGCTG**CTCAAATGCGGCTTC
	AluI
R65K	TTCCGCCATCGTC**AGCTT**CTCAAATGCGGCTTC

[a] Restriction enzyme sites are denoted by the bold letters. Restriction sites in parentheses indicate that the restriction enzyme cleaves the wild-type plasmid DNA but not the mutant.

Product inhibition by GDP and the low activities of H124Q, H88Q, E70Q, R52Q, and R65Q mutants were measured using a tritiated GDP-mannose substrate as previously described (*8*). The ^{3}H label was at the C2′ of the mannose moiety of the substrate.

Kinetic Studies of Mn^{2+} and Mg^{2+} Activation. The effects of varying metal and substrate concentrations on the initial rates of GDP-mannose hydrolysis were measured at 22 °C with 80 mM Na^+ HEPES buffer, pH 7.5. The kinetic data were simultaneously fit to a general rate equation for a metal-activated enzyme with a random order mechanism (eq 3) to

Scheme 1

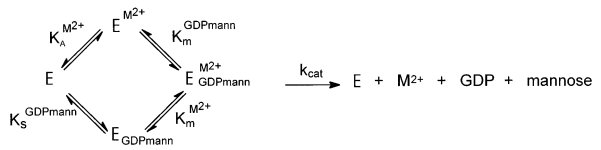

evaluate the five kinetic parameters defined in Scheme 1, as was previously done for the wild-type enzyme (*8*):

$$v = (V_{max}[M^{2+}][\text{GDP-mannose}]_{Free})/ (\beta K_a^{M2+} K_s^{GDPmann} + \beta K_a^{M2+}[\text{GDP-mannose}]_{Free} + \beta K_s^{GDPmann}[M^{2+}] + [M^{2+}][\text{GDP-mannose}]_{Free}) \quad (3)$$

In eq 3, β is a proportionality constant used in describing the following relationships for the thermodynamic box in Scheme 1:

$$K_m^{M2+} = \beta K_a^{M2+} \quad (4)$$

$$K_m^{GDPmann} = \beta K_S^{GDPmann} \quad (5)$$

Activation by Mn^{2+} was measured at 0.2, 0.6, 1.2, and 6.0 mM $MnCl_2$ at 22 °C, pH 7.5, during a 20 min assay period for the E64Q mutant. The GDP-mannose concentration was also varied (0.19, 0.38, 1.52, and 5.33 mM). Other components present were 80 mM Na^+ HEPES pH 7.5 and approximately 1−2 mU of GDPMH in a 50 μL total volume. The reactions were stopped by heating at 95 °C for 3 min, followed by a 2 min incubation on ice. One unit of calf intestinal alkaline phosphatase was added and the reactions were incubated for 11 min at 37 °C. EDTA (250 μL of a 5 mM solution) and 700 μL of Ames Mix (6 parts 0.42% ammonium molybdate in 1 N H_2SO_4 and 1 part 10% ascorbic acid) were added, and the solutions were heated for 30 min at 37 °C. The concentration of phosphomolybdate was measured at 780 nm using potassium phosphate as a standard. Similarly, activation by Mg^{2+} of the E64Q mutant was measured at 0.2, 0.6, 1.2, and 6.0 mM $MgCl_2$ at 22 °C, pH 7.5 during a 20 min assay period. The GDP-mannose substrate concentration was varied (0.2, 0.4, 1.6, and 5.6 mM).

Activation by Mn^{2+} of the E60Q mutant was measured at pH 7.5 and 22 °C using the standard assay. The K_m^{Mn2+} was measured at two saturating concentrations of GDP-mannose, 2.02 and 3.36 mM. The concentrations of $MnCl_2$ were 0.02, 0.04, 0.06, 0.08, 0.10, 0.12, 0.14, and 0.20 mM. Activation by Mg^{2+} was measured at two saturating concentrations of GDP-mannose, 3.3 and 7.7 mM, using the standard assay at pH 7.5 and 22 °C. The concentrations of $MgCl_2$ were 0.2, 0.4, 0.8, 1.2, 1.6, and 2.0 mM.

Activation by Mn^{2+} of the H142Q mutant was measured at 0.002, 0.006, 0.010, 0.012, 0.014, and 0.016 mM $MnCl_2$ with varying GDP-mannose concentrations of 0.23, 0.46, 0.92 1.84, and 3.45 mM at pH 7.5, 22 °C. The concentrations of Mg^{2+} and GDP-mannose used to measure kinetic constants of Mg^{2+} activation of the H142Q mutant were similar to those used with the E64Q and E60Q mutants.

Mn^{2+} Binding Studies of the E70Q Mutant. The metal binding stoichiometry and dissociation constant of Mn^{2+} from the ternary enzyme−Mn^{2+}−GDP complex were determined by Scatchard analysis. The concentration of free Mn^{2+} in a mixture of free and bound Mn^{2+} was measured by EPR at 22 °C in the presence of 80 mM Na^+ HEPES pH 7.5 on a Varian E-4 EPR spectrometer operating at X-band (9.1 GHz), as previously described (*8*). Bound Mn^{2+} was monitored by the longitudinal proton relaxation rate of water, $1/T_1$. A $180°-\tau-90°$ pulse sequence was used to measure $1/T_1$ of bulk water protons. PRR data were collected using a Seimco pulsed NMR spectrometer operating at 24.3 MHz as previously described (*8*). Samples volumes were 40 μL and contained 50.6 μM E70Q enzyme subunits and 49.5 μM GDP or 101.1 μM E70Q enzyme subunits and 99.0 μM GDP. Also present was 80 mM Na^+ HEPES pH 7.5. The $MnCl_2$ concentration was varied between 51 μM and 1.00 mM.

$^1H-^{15}N$ HSQC Spectral Titrations of the E70Q Mutant with $MnCl_2$. To determine the relative distance of the Gln-70 side chain NH_2 resonances from the paramagnetic active site Mn^{2+} ion, we titrated $MnCl_2$ (0.088 μM to 62.28 μM) into an initial solution containing 0.98 mM E70Q enzyme subunits in the presence of an initial concentration of 0.973 mM GDP, in 11 steps. Other components present were 5.4 mM d_{11} Tris-HCl, pH 7.5, 0.3 mM NaN_3, 18 mM NaCl, 10 mM DTT, 0.1 mg/mL AEBSF, and 10% D_2O. $^1H-^{15}N$ HSQC spectra were collected at 21.5 °C as previously described (*8*) on a Varian Unity Plus 600 MHz NMR spectrometer equipped with a Varian 5 mm triple-resonance probe with an actively shielded *Z*-gradient. The data were collected using States-TPPI in the indirect dimension with spectral widths of 2000 Hz (^{15}N, t_1, 100 points) and 8000 Hz (^1H, t_2, 1024 points).

Cross-peak volumes were corrected for the small dilution of the enzyme over the course of the titration. The concentration of Mn^{2+} which reduced the peak volume by 50%, $[Mn^{2+}]_{1/2}$, was calculated from the slope of the line relating peak volume to Mn^{2+} concentration. Assuming that the loss of signal volume is dominated by paramagnetic effects on transverse relaxation rates ($1/T_{2p}$) for each affected NH cross-peak, we calculated the relative Mn^{2+} to ^{15}N distances as proportional to the sixth root of the respective $[Mn^{2+}]_{1/2}$ values (*7*, *11*).

Effects of pH on the Kinetic Parameters of Wild Type and Mutants of GDPMH. For all kinetic measurements of pK_a, Na^+ MES buffer was used for pH values of 6.0, 6.3, 6.5, and 7.0, Tris-HCl buffer was used at pH 7.0, 7.5, 8.0, and 8.5, and Na^+ glycine buffer was used at pH 8.5, 9.0, 9.3, 9.5, and 10.0. The k_{cat} and K_m of the wild-type enzyme were measured at nine pH values (6.0, 6.3, 6.5, 7, 7.74, 8, 8.5, 9, 9.5). The k_{cat} of the E64Q mutant at 37 °C was measured at two saturating concentrations of GDP-mannose, 9.94 and 12.42 mM, and at eight pH values (6.0, 6.5, 7.0, 7.5, 8.0, 8.5, 9.0, and 9.5). The k_{cat} of the E60Q mutant was measured at 2.46 and 5.96 mM GDP-mannose at 10 pH values (6.0, 6.3, 6.5, 7.0, 7.5, 8.0, 8.5, 9.0, 9.3, and 9.8) and the k_{cat} of the H124Q mutant was measured at 4.56 mM GDP-mannose at 10 pH values (6.0, 6.3, 6.5, 7.0, 7.5, 8.0, 8.5, 9.0, 9.3, and 10.0). The k_{cat} of the H88Q mutant was measured at 3.34 and 6.68 mM GDP-mannose at 10 pH values (6.4, 6.6, 6.8, 7.0, 7.5, 8.0, 8.5, 9.0, 9.4, and 10.0).

Effects of Increasing Ionic Strength on the Kinetically Determined pK_a. The pK_a in k_{cat} versus pH for wild-type GDPMH was measured using the standard assay with an

additional 0.0, 100, 200, or 300 mM NaCl at pH values 6.0, 6.3, 6.5, 7.0, 7.5, 8.0, and 8.5 at 37 °C.

Temperature Dependence of the Kinetically Determined pK_a. A van't Hoff plot was constructed for wild-type GDPMH. The pK_a in k_{cat} was measured at 4, 22, 28, and 37 °C using the standard assay at 10 pH values between pH 6.0 and 10.0. The pH values of each of the buffers in the presence of 20 mM $MgCl_2$ were measured at the four temperatures. The slope of the pK_a versus 1000/T yielded the $\Delta H^{ionization}$ for the GDPMH enzyme.

pH Titrations of the Histidine Residues of Wild-Type GDPMH. Chemical shift changes in the imidazole ring $^{15}N\delta$, $^{15}N\epsilon$, $^{1}H\delta C$, and $^{1}H\epsilon C$ resonances of the histidine residues as a function of pH were monitored by two-dimensional $^{1}H-^{15}N$ HSQC spectra of the histidine imidazole region using ^{15}N-labeled GDPMH (*20*, *21*) at 28 °C. Spectral widths of 6078 Hz centered at 210 ppm in the ^{15}N dimension and 6000 Hz centered at 4.74 ppm in the proton dimension were used. A total of 100 points were used in t_1, and 1024 points were used in t_2. From the HSQC spectra, the protonation state of each histidine was identified (*20*). As noted (*20*), the intensities of the cross-peaks were proportional to $\sin^2(\pi J\tau)$, where τ, the $^{1}H-^{15}N$ mixing period, was set to 22 ms. To sequence-specifically assign the resonances of the four histidines of GDPMH, we also collected individual $^{1}H-^{15}N$ HSQC spectra on three ^{15}N-labeled mutants, H88Q, H124Q, and H142Q. Although not required to complete the assignments, an attempt to collect a 2D spectrum of the H102Q mutant was unsuccessful due to aggregation.

To determine the pK_a values of the histidines, we collected eight complete two-dimensional $^{1}H-^{15}N$ HSQC spectra at 28 °C, at pH 6.12, 6.38, 7.00, 7.30, 7.57, 7.73, 8.13, and 8.93 in 90% H_2O, 10% D_2O, and 72 mM Na^+ HEPES.

The pH titration data were fit to eq 6

$$\Delta\delta = \frac{\delta_1 + \delta_2(10^{pH-pKa})^n}{(10^{pH-pKa})^n + 1} \quad (6)$$

to yield the low pH (δ_1) and high pH (δ_2) limits for the chemical shift change during the titration, the Hill coefficient (n), and the pK_a.

Because collection of each $^{1}H-^{15}N$ HSQC spectrum took 2.5 h, an independent and accelerated pH titration of wild-type GDPMH was also carried out by collecting only the first 8 FIDs (real and imaginary) of the 2D $^{1}H-^{15}N$ HSQC spectrum, which required only 24 min, at each pH (6.15, 6.35, 6.49, 6.60, 6.85, 7.09, 7.29, 7.46, 7.67, 7.89, 8.09, 8.31, and 8.82). Fourier transformation of the individual FIDs in the ^{1}H dimension showed eight well-resolved proton resonances with no interfering signals from the backbone NH groups. The phase of each proton resonance varied periodically among the individual spectra, depending on the ^{15}N evolution time (t_1) and also on the chemical shifts of the proton resonances. Hence, for each pH, one of the eight spectral increments (slices) was chosen on the basis of signal/noise to measure the chemical shifts of the $H\epsilon C$ protons. The $H\epsilon C$ chemical shifts of His-88 and of His-124 in these 1D slices were identified by collecting identical spectra of the ^{15}N-labeled H88Q and H124Q mutant enzymes in 10% D_2O, 72 mM Na^+ HEPES, pH 7.5, at 28 °C.

As an additional, independent check of the titration parameters of His-124, the standard method of one-dimensional proton NMR in 99% D_2O, was used (*22*). Unlabeled wild-type enzyme (0.95 mM) was exchanged into 99.9% D_2O, 72 mM Na^+ HEPES by ultrafiltration, as previously described (*5*, *8*), and stored at 4 °C for 3 days to allow for complete exchange of backbone NH groups. One-dimensional proton spectra were collected at 28 °C at pH 5.82, 6.35, 6.59, 6.77, 7.04, 7.15, 7.27, 7.42, 7.52, 7.67, 7.86, and 8.03. Approximately 700 transients were collected at each pH. One-dimensional proton spectra of the H88Q and H124Q mutants were also collected at pH 7.0 and 7.5 in 99% D_2O and 72 mM HEPES to identify these resonances.

$^{1}H-^{15}N$ HSQC Spectral Titrations of R52Q with Mg^{2+}. The R52Q mutant (1.22 mM subunits) was titrated with 0.0−20.34 mM $MgCl_2$ in eight steps. Five cross-peaks were followed during the course of the titration with chemical shift changes greater than 0.08 ppm in the proton dimension and were used to calculate an average dissociation constant. The GDP product was then titrated in eight steps (0.0−11.48 mM) into the sample which contained 0.93 mM R52Q and 20.34 mM $MgCl_2$. A titrant containing equimolar concentrations of $MgCl_2$ and GDP was used to maintain the free Mg^{2+} at a constant concentration.

$^{1}H-^{15}N$ HSQC and Three-Dimensional $^{15}N-$HSQC−NOESY Spectra. Two-dimensional $^{1}H-^{15}N$ HSQC spectra were collected for all mutants as previously described (*8*) and compared with that of the wild-type enzyme to assess changes in structure. Although all of the $^{1}H-^{15}N$ peaks are currently unassigned, each peak could be identified by its spin system in a three-dimensional $^{15}N-$HSQC−NOESY experiment. Spectra were acquired at 600 MHz using a 75 ms mixing time at 28 °C. Spectral widths were 8700 Hz (^{1}H, t_3, 1024 points), 8000 Hz (^{1}H, t_1, 100 points), and 2000 Hz (^{15}N, t_2, 64 points), using 16 transients per hypercomplex t_1 and t_2. Each three-dimensional experiment took approximately 60 h to acquire. The ^{15}N-labeled mutants (approximately 1 mM in subunit concentration), with the exception of H88Q and H124Q, were present together with 5.4 mM d_{11} Tris HCl pH 7.5, 0.3 mM sodium azide, 10% D_2O, 18 mM NaCl, 10 mM DTT, and 0.1 mg/mL AEBSF. To avoid precipitation, we studied the H88Q and H124Q mutants in the presence of 72 mM HEPES pH 7.5, 0.1 mg/mL AEBSF, 10% D_2O, and 0.3 mM sodium azide at 28 °C. Spectra of the wild-type enzyme collected in both buffering systems showed no significant differences. Under these conditions, wild-type GDPMH and all of the mutant enzymes except for the H102Q mutant were stable and did not precipitate during the course of the experiments.

Search for Disaccharide Formation by GDPMH. Thin-layer chromatography (*23*) was used to search for disaccharide formation in the standard GDPMH assay, to which was added 30 mM D-glucose, D-fucose, L-fucose, L-rhamnose, *N*-acetyl-D-glucosamine, D-glucosamine, or D-mannose. The developing solution was 3:1 2-propanol:aqueous Na Borate (10 g/L). A second developing solution which improved resolution contained 3:1:4 2-propanol:Na Borate (10 g/L):butanol.

RESULTS

Effect of pH on k_{cat} and $k_{cat}/K_m^{GDPmann}$. GDPMH has previously been shown to require a single divalent cation

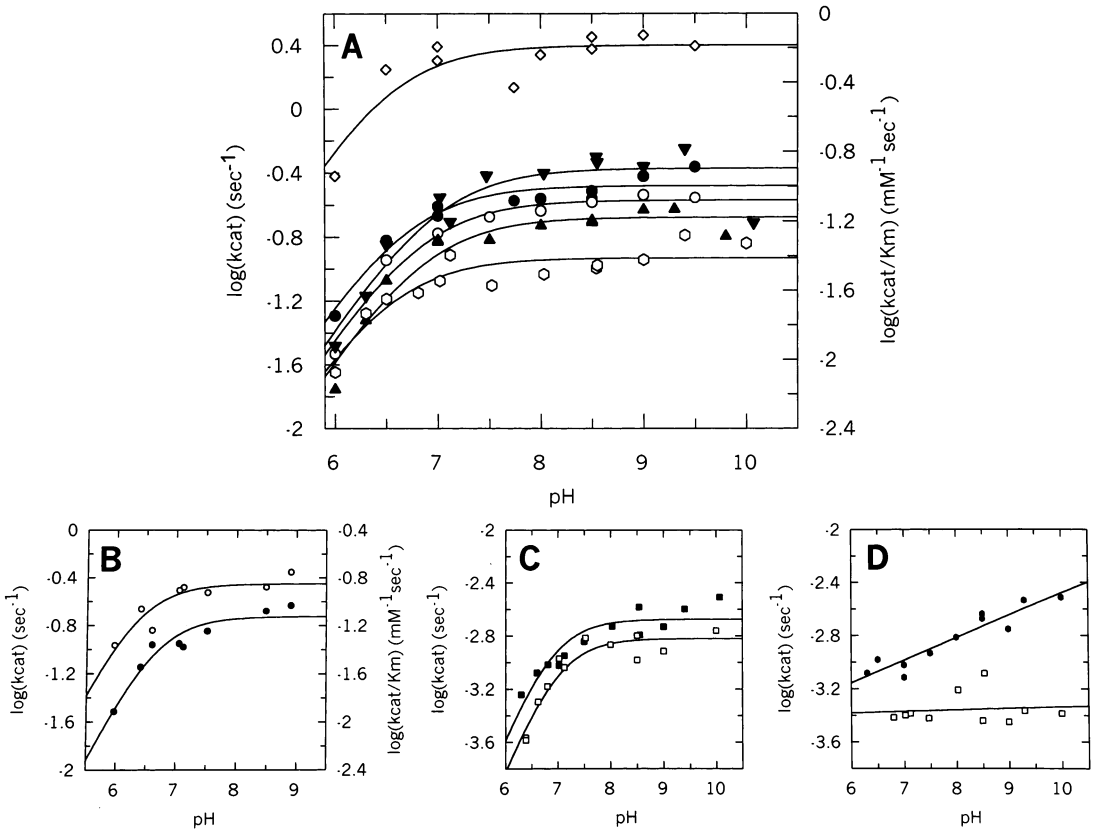

FIGURE 2: pH dependence of kinetic parameters for the wild-type enzyme and mutants of GDPMH. Buffers used are stated in the text. (A) pH dependence of k_{cat} (●) and k_{cat}/K_m (◇) of the wild-type enzyme, pH dependence of k_{cat} of the E64Q (○), E60Q (▲), H102Q (▼), and H142Q (⬡) mutants at 37 °C. The initial slope of the wild-type curve was 0.95, corresponding to ~1.0 deprotonation. (B) pH dependence of k_{cat} (●) and k_{cat}/K_m (○) of wild-type enzyme at 28 °C. (C) Measurement of the pK_a of the H88Q mutant at 28 °C (□) and 37 °C (■). (D) Effect of pH on k_{cat} of the H124Q mutant at 37 °C (⬢) and at 28 °C (□). The linear increase at 37 °C is proportional to $[OH]^{0.17}$.

Table 2: Kinetic Constants of Wild-Type GDPMH and Mutants at pH 9.3 and 37 °C with Mg^{2+} Activation

enzyme	V_{max} (U/mg)	k_{cat} (s^{-1})	$K_m^{GDP-mann}$ (mM)	fold decrease in k_{cat}	p$K_{HESMg^{2+}}$[a]
WT	2.3 ± 0.3	0.71 ± 0.09	0.32 ± 0.06	1.00	6.70 ± 0.06[b] 6.38 ± 0.20[c]
E64Q	2.10 ± 0.06	0.64 ± 0.02	0.28 ± 0.05	1.11	6.82 ± 0.06
A69E	0.78 ± 0.06	0.24 ± 0.08	1.19 ± 0.09	3.0	
E60Q	1.5 ± 0.2	0.46 ± 0.06	2.4 ± 0.3	1.5	6.85 ± 0.08
E70Q	0.016 ± 0.003	0.0049 ± 0.0009	3.2 ± 0.6	$10^{2.2}$	6.87 ± 0.25
H88Q	0.0116 ± 0.0009	0.0036 ± 0.0003	1.4 ± 0.3	$10^{2.3}$	6.86 ± 0.11
H102Q	0.3 ± 0.1	0.09 ± 0.03	4.4 ± 1.3	7.9	6.97 ± 0.12
H124Q	0.0010 ± 0.0002	0.00031 ± 0.00006	1.5 ± 0.4	$10^{3.4}$	d
H142Q	1.7 ± 0.2	0.52 ±0.06	0.9 ± 0.1	1.4	6.52 ± 0.10
R52Q	0.007 ± 0.002	0.0023 ± 0.0005	13 ± 3	$10^{2.5}$	
R52K	0.2 ± 0.1	0.06 ± 0.04	14 ± 2	11.8	
R65Q	0.08 ± 0.05	0.03 ± 0.01	26 ± 15	23.6	
R65K	0.18 ± 0.04	0.06 ± 0.01	1.1 ± 0.2	11.8	

[a] Determined from the effect of pH on k_{cat}. [b] p$K_{HESMg^{2+}}$ is 6.60 ± 0.08 at 28 °C. [c] pK_{HEMg2+}, determined from the effect of pH on k_{cat}/K_m, is 6.40 ± 0.20 at 28 °C. [d] No pK_a detected; k_{cat} increased with $[OH^-]^{0.17}$.

for activity which bridges the enzyme to the GDP product (*8*). Mechanistically, in addition to the divalent cation, GDPMH probably also requires a general base catalyst to deprotonate the attacking water[2] and an additional electrostatic catalyst to further activate the departure of the leaving group. With wild-type GDPMH at saturating concentrations of Mg^{2+} (20 mM), the log($k_{cat}/K_m^{GDPmann}$) increased with pH with unit slope, showing a pK_a of 6.38 ± 0.20 at 37 °C, followed by a plateau between pH 8.0 and pH 9.5, above which the enzyme denatured (Figure 2A). At saturating substrate, log(k_{cat}) showed similar behavior with pH, however, with a slightly higher pK_a value of 6.70 ± 0.06 (Figure 2A, Table 2). Hence, a group on the enzyme−Mg^{2+} complex, essential for activity, shows a pK_a of 6.4, which increases to 6.7 when GDP-mannose binds. Because the enzyme was saturated with Mg^{2+} in this experiment, this pK_a is likely to be that of the general base, rather than that of a metal ligand.

Properties of the E70Q Mutant. In a search for metal ligands, as well as general base and electrostatic catalysts, mutations were made on the basis of catalytic residues found in the homologous MutT enzyme (*6*, *7*).[6] The k_{cat} and $K_m^{GDPmann}$ were determined for all mutants at 37 °C and at the pH optimum (pH 9.3) where the wild-type enzyme is maximally active. Glu-70 of GDPMH corresponds to an

Table 3: Kinetic Constants Determined at pH 7.5 and 22 °C with Mn^{2+} and Mg^{2+} Activation[a]

enzyme	metal	K_a^{M2+} (mM)	K_m^{M2+} (mM)	$K_s^{GDPmann}$ (mM)	$K_m^{GDPmann}$ (mM)	K_I^{GDP} (mM)	k_{cat} (s^{-1})
wt	Mn^{2+}	3.86 ± 1.12	0.32 ± 0.18	1.9 ± 0.5	0.16 ± 0.09	0.046 ± 0.027[b]	0.15 ± 0.01
wt	Mg^{2+}	3.90 ± 1.32	0.69 ± 0.42	1.4 ± 0.4	0.24 ± 0.14	0.056 ± 0.023[b]	0.13 ± 0.01
E70Q	Mg^{2+}	–	13.9 ± 2.1	–	–	–	0.0025 ± 0.0003
E64Q	Mn^{2+}	2.88 ± 0.60	0.22 ± 0.07	2.2 ± 0.5	0.17 ± 0.05	0.064 ± 0.028[b]	0.31 ± 0.02
E64Q	Mg^{2+}	2.66 ± 0.86	0.82 ± 0.48	0.82 ± 0.28	0.27 ± 0.15	–	0.21 ± 0.02
A69E	Mn^{2+}	5.59 ± 1.92	0.32 ± 0.20	3.0 ± 0.8	0.17 ± 0.10	0.021 ± 0.003	0.10 ± 0.007
A69E	Mg^{2+}	4.58 ± 1.77	0.52 ± 0.37	2.2 ± 0.7	0.25 ± 0.17	0.023 ± 0.009	0.08 ± 0.006
E60Q	Mn^{2+}	–	0.046 ± 0.005	–	0.80 ± 0.24	–	0.113 ± 0.003
E60Q	Mg^{2+}	–	0.41 ± 0.11	–	0.27 ± 0.02	–	0.054 ± 0.009
H142Q	Mn^{2+}	0.2 ± 0.1	0.003 ± 0.002	2.1 ± 0.3	0.03 ± 0.01	–	0.07 ± 0.004
H142Q	Mg^{2+}	6.3 ± 2.7	0.73 ± 0.55	1.6 ± 0.5	0.19 ± 0.09	–	0.098 ± 0.005

[a] Kinetic constants are defined in Scheme 1. [b] Determined by radioactive assay.

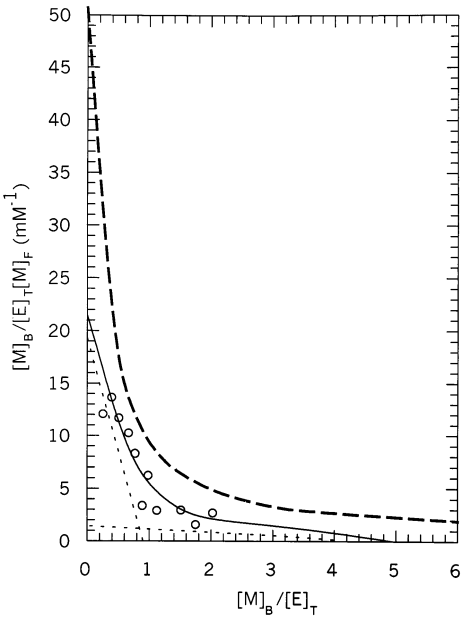

FIGURE 3: Scatchard plot of Mn^{2+} binding to the GDP complex of the E70Q mutant of GDPMH. The dotted lines show the contributions of the tight and weak Mn^{2+} binding sites. Stoichiometries and dissociation constants are given in the text. The Scatchard plot for wild-type GDPMH is shown as a heavy dashed line for comparison (8).

important metal liganding residue in MutT, Glu-57 (*7*). In GDPMH, the Mg^{2+}-activated E70Q mutant at pH 9.3 and 37 °C showed a large $10^{2.2}$-fold decrease in k_{cat} and a 10-fold increase in the $K_m^{GDPmann}$ of the substrate (Table 2). The effect of pH on k_{cat} yielded a pK_a of 6.87 ± 0.25, overlapping with that of the wild type, but the errors were large because of the low activity (Table 2). Under conditions in which the metal-binding properties of the wild-type enzyme were studied, pH 7.5 and 22 °C (*8*), the kinetically determined dissociation constant of Mg^{2+} from the E70Q mutant at high (6.82 mM) substrate concentration was found to be 13.9 ± 2.1 mM, 20-fold greater than that of the wild-type enzyme (Table 3), suggesting that Glu-70 functions as a metal ligand.

Direct binding of Mn^{2+} to the enzyme−GDP complex, monitored by EPR and by water proton relaxation rates, yielded a dissociation constant for Mn^{2+} from the ternary E−Mn^{2+}−GDP complex of the wild-type enzyme, $K_A' = 15 \pm 3$ μM (Figure 3) (*8*). The mutation of Glu-70 to Gln increased K_A' 3-fold to a value of 45 ± 5 μM (Figure 3). Similar 3-fold weakening of Mn^{2+} and Mg^{2+} binding was found in the E57Q mutant of the MutT enzyme (*7*). The dissociation constants of the nonspecific, weakly bound Mn^{2+} ions in the enzyme−Mn^{2+}−GDP ternary complex of the E70Q mutant ($n \sim 4$, $K_A^{Mn2+} = 2.9 \pm 0.8$ mM) did not significantly differ from those of the wild-type enzyme (*8*), suggesting these sites to be unperturbed by the mutation (Figure 3). A more accurate determination of the number of weak Mn^{2+} binding sites on the enzyme was not obtainable due to the larger errors in binding data obtained at high Mn^{2+} concentrations.

Another parameter obtained from Mn^{2+} binding studies is the enhancement factor (ϵ_T) for the effect of Mn^{2+} in the ternary E−Mn^{2+}−GDP complex on the $1/T_1$ of water protons. The value of ϵ_T for the E70Q mutant (3.8 ± 0.2) is significantly lower than that of the wild-type enzyme (4.9 ± 0.4) (*8*), indicating a structural change in the coordination sphere of Mn^{2+}.

Two new side chain NH_2 resonances of Gln-70 were identified in $^1H-^{15}N$ HSQC spectra of the E70Q mutant with proton chemical shifts at 7.21 and 6.97 ppm and an ^{15}N chemical shift at 114.3 ppm (Table S1, Supporting Information). Very strong paramagnetic effects on these two side chain NH_2 cross-peaks were observed in a $^1H-^{15}N$ HSQC Mn^{2+} titration of the E70Q mutant (0.98 mM subunits) with $MnCl_2$ (0.088−62.3 μM) in the presence of 0.97 mM GDP, revealing the close proximity of the Gln-70 $-NH_2$ side chain to the active site Mn^{2+} ion (Figure 4). Strong to moderate paramagnetic effects were also observed on other resonances in the $^1H-^{15}N$ HSQC spectra which were not assigned (Figure 4), yielding the relative distances given in Table S1. Of the 15 backbone NH signals on which strong to moderate paramagnetic effects were detected, Gln-70 NH_a and Gln-70 NH_b showed distances to Mn^{2+} only 1.12- and 1.19-fold greater than that of the closest NH group (Table S1).

Perturbations of the structure of the E70Q mutant were assessed by measuring chemical shift differences in the $^1H-^{15}N$ HSQC spectra from those of the wild-type enzyme. The $^1H-^{15}N$ HSQC spectra of the E70Q mutant showed only 22 peaks out of 171 which differed by more than 0.5 ppm from wild type in the ^{15}N dimension and 30 peaks which differed by more than 0.05 ppm from wild type in the proton dimension. NOESY spectra showed only small changes in NOE data. Therefore, the E70Q mutation did not greatly alter the structure of the enzyme.

Glutamate and Related Residues Playing Minor Roles. Glu-60 is not conserved among all Nudix enzymes but is present in MutT as Glu-47, the first residue of helix I (*11*), which it may help stabilize (Figure 1).[6] A very small 1.5-fold decrease in the k_{cat} was observed at 37 °C, pH 9.3, upon removal of this negatively charged residue in the E60Q

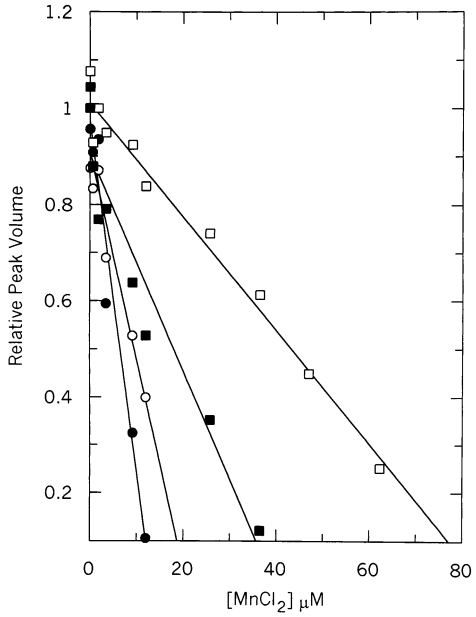

FIGURE 4: Paramagnetic effects of Mn^{2+} on the resonances of the $^1H-^{15}N$ HSQC spectrum of the E70Q mutant of GDPMH at 21 °C, pH 7.5. Solutions contained 0.98 mM GDPMH subunits and 0.97 mM GDP. Other components present were 5.4 mM d_{11} Tris, 18 mM NaCl, 10 mM DTT, 0.1 mg/mL AEBSF, 10% D_2O, and 0.3 mM sodium azide. The symbols (○) and (●) are the assigned Q70 NH_2 resonances at 7.21 and 114.3 and at 6.97 and 114.35 ppm, respectively. Two other unassigned resonances further away from the Mn^{2+} ion are shown at (□) 8.66 and 130.84 ppm and (■) 8.00 and 106.81 ppm.

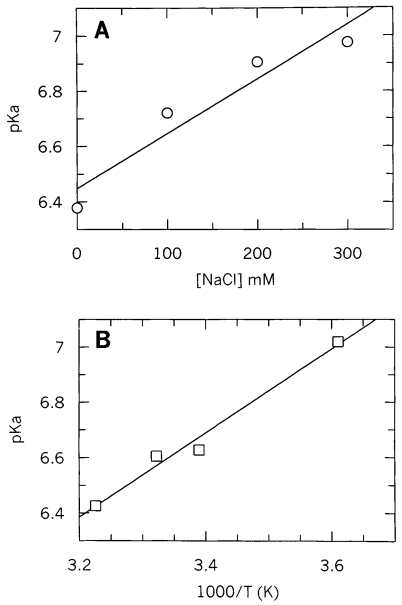

FIGURE 5: Effects of ionic strength and temperature on the single deprotonation observed in the plot of pH vs log(k_{cat}). (A) Effect on the pK_a of the wild-type GDPMH enzyme of increasing ionic strength (0, 100, 200, and 300 mM NaCl) at 37 °C. Other components present in the assays were 80 mM buffer (MES was used at pH 6.0, 6.3, 6.5, 6.7 ,and 7.0, Tris-HCl was used at pH 7.0, 7.5, 8.0, and 8.5, or Na^+ glycine was used at pH 8.5, 9.0, 9.3, and 10.0) and 20 mM $MgCl_2$. (B) van't Hoff plot showing the effect of temperature on the kinetically determined pK_a from pH vs k_{cat} studies. The pK_a was measured at four temperatures, 4, 22, 28, and 37 °C, for the wild-type GDPMH enzyme. The slope of the line equals $\Delta H^{ionization}/(2.3R)$, which leads to $\Delta H^{ionization} = 7.0 \pm 0.67$ kcal/mol.

mutant of GDPMH (Table 2). The $K_m^{GDPmann}$ of the substrate in the presence of a saturating concentration of Mg^{2+} ($K_m^{GDPmann} = 2.4 \pm 0.3$ mM) at 37 °C and pH 9.3 increased 7.5-fold (Table 2). An unexpected 7-fold decrease in the K_m of Mn^{2+} was detected kinetically ($K_m^{Mn^{2+}}$ (E60Q) = 0.046 ± 0.005 mM) in comparison with that of the wild-type enzyme at 22 °C at pH 7.5 (Table 3), but no significant change in affinity for the Mg^{2+} ion was observed. The effect of pH on k_{cat} of the E60Q mutant yielded a pK_a = 6.85 ± 0.08, which was similar to that of the wild-type enzyme (6.70 ± 0.06) at 37 °C (Figure 2A, Table 2), arguing against the role of Glu-60 as a general base.

Glu-64 precedes rather than follows Arg-65 in GDPMH, unlike all other Nudix enzymes, which have the conserved sequence RE (Figure 1). In the MutT enzyme, Glu-53 is a reversible ligand to the enzyme-bound divalent cation in the free enzyme, which dissociates from the metal in the enzyme−substrate complex to function as the general base (*6*). In the E64Q mutant of GDPMH, the k_{cat} and $K_m^{GDPmann}$ were in close agreement with the corresponding kinetic parameters of the wild-type enzyme (Table 2). Kinetically measured dissociation constants of the metal extrapolated to zero and infinite substrate concentrations and of the substrate extrapolated to zero and infinite metal concentrations were also not significantly different from those of the wild-type enzyme (Table 3), indicating that Glu-64 does not act as a metal ligand or general base in GDPMH. Accordingly, the pH dependence of k_{cat} of the E64Q mutant, with a pK_a = 6.82 ± 0.06, was very similar to that of the wild-type enzyme (6.70 ± 0.06) (Figure 2, Table 2). The $^1H-^{15}N$ HSQC spectrum of the E64Q mutant showed only 22 of 171 peaks differing in proton chemical shifts by more than 0.05 ppm from the wild-type enzyme and five peaks differing in ^{15}N chemical shifts by more than 0.5 ppm from the wild-type enzyme. The $^{15}N-$HSQC−NOESY spectrum differed little from that of the wild-type enzyme. Hence, the E64Q mutation did not significantly perturb the structure or function of the enzyme.

The Ala-69 residue in GDPMH corresponds to a metal ligand, Glu-56, in MutT.[6] In the A69E mutant of GDPMH, a moderate 3.7-fold increase in the K_m of the substrate ($K_m^{GDPmann} = 1.19 \pm 0.09$ mM) and a 3.0-fold decrease in the k_{cat} were observed at pH 9.3 and 37 °C (Table 2). The kinetically measured dissociation constants of the substrate extrapolated to zero and infinite metal concentrations and of the Mn^{2+} and Mg^{2+} ions extrapolated to zero and infinite substrate concentrations (Table 3) were within error of the kinetically measured dissociation constants of the wild-type enzyme. Hence, incorporation of a glutamate at this position had no effect on the affinity for the metal ion indicating that Glu-69 does not function as a metal ligand.

Effects of Ionic Strength and Temperature on the Kinetically Measured pK_a. Since none of the Glu residues corresponding to those in helix I of MutT functioned as a general base and because of the high pK_a value of 6.70 ± 0.06 in the effect of pH on k_{cat} (Table 2), the possibility of a neutral histidine as general base was explored. Wild-type GDPMH showed an increase in the kinetically measured pK_a with increasing ionic strength (Figure 5A), consistent with a required deprotonation of a cationic histidine residue or a terminal $-NH_3^+$ group. Increasing the ionic strength would have the opposite effect on a Glu or Asp residue. A decrease

in pK_a with increasing temperature was also consistent with the deprotonation of a cationic nitrogen (Figure 5B). The van't Hoff plot yields a slope equal to $\Delta H/(2.3R)$. The heat of ionization of the residue affecting k_{cat} of GDPMH was found to be 7.00 ± 0.67 kcal/mol (Figure 5B), consistent with the $\Delta H^{ionization}$ of a solvent-exposed histidine residue (6.9−7.5 kcal/mol). The $\Delta H^{ionization}$ of a solvent-exposed glutamate is 0 ± 1.5 kcal/mol (*24*, *25*). GDPMH contains four histidine residues (His-88, 102, 124, and 142), and each was individually mutated to Gln to determine if one was responsible for the single deprotonation.

Properties of the H88Q Mutant. Mutation of His-88 to Gln resulted in a $10^{2.3}$-fold decrease in the k_{cat} and a 4.4-fold increase in the K_m of the GDP-mannose substrate (Table 2), indicating that His-88 was important to the structure or mechanism of GDPMH. However, the effect of pH on k_{cat} (Figure 2C) yielded a pK_a of 6.86 ± 0.11 for the H88Q mutant, similar to that of the wild-type enzyme, indicating that His-88 is not functioning as the general base. A structural role for His-88 is possible since small structural perturbations were observed in the H88Q mutant by the analysis of changes in chemical shifts in the $^1H-^{15}N$ HSQC spectra of the mutant. Thus, 48 of 171 peaks differed by more than 0.05 ppm in the proton dimension and 27 of 171 peaks differed in the ^{15}N-dimension by more than 0.5 ppm from the wild-type enzyme.

Properties of the H102Q Mutant. Mutation of His-102 to Gln resulted in a 7.9-fold decrease in k_{cat} and a 13.8-fold increase in the $K_m^{GDPmann}$ (Table 2), suggesting a modest role of His-102 in structure and/or catalysis. The effect of pH on k_{cat} yielded a pK_a of 6.97 ± 0.12, similar to that of the wild-type enzyme (Table 2). Because of its aggregation at millimolar concentrations, no structural studies were made.

Properties of the H124Q Mutant. Mutation of His-124 to Gln resulted in the largest decrease in the k_{cat} of the histidine mutants ($10^{3.4}$-fold) and a 4.7-fold increase in the $K_m^{GDPmann}$ (Table 2). The pK_a in the effect of pH on log(k_{cat}) was lost in the H124Q mutant. Instead, a small linear increase in log(k_{cat}) proportional to $[OH^-]^{0.17}$ was observed at 37 °C (Figure 2D), suggesting that OH^- is now contributing slightly to base catalysis. This small increase in log(k_{cat}) with pH was not detected at 28 °C, where the activity was lower and the errors in k_{cat} were greater.

The structure of the H124Q mutant was not significantly different from that of the wild-type enzyme based upon chemical shift changes observed in the $^1H-^{15}N$ HSQC spectra of the mutant. Only 15 of 171 peaks differed in chemical shift by more than 0.05 ppm in the proton dimension, and five peaks differed by more than 0.5 ppm in the ^{15}N dimension. The data thus show that His-124 functions only when it is deprotonated and that it can be partially replaced by OH^-, indicating His-124 to be the general base.

Properties of the H142Q Mutant. The H142Q mutation resulted in a small 1.4-fold decrease in k_{cat} and a 2.8-fold increase in the $K_m^{GDPmann}$ (Table 2). The metal binding properties of the H142Q mutant were also studied. A large 100-fold decrease in the K_m^{Mn2+} to 3 ± 2 μM was found, while the K_m^{Mg2+} = 0.7 ± 0.5 mM was identical to that of the wild-type enzyme (Table 3). The activity of this mutant was approximately 2.1-fold lower than that of wild-type GDPMH when activated by Mn^{2+} and only 1.3-fold lower than the wild-type enzyme when activated by Mg^{2+} (Table 3), indicating that His-142 is not an essential catalytic residue. The pK_a found for the H142Q mutant was not significantly different from that found for the wild-type enzyme (Table 2).

Determination of the State of Protonation of Histidine Residues of GDPMH by NMR. $^1H-^{15}N$ HSQC spectra of wild-type GDPMH and of the Gln mutants of three of the four histidine residues, H88Q, H124Q, and H142Q, permitted the unequivocal assignment of the four histidines and their states of protonation at pH 6.1 and 28 °C (Figure 6, Table 4). The H102Q mutant aggregated, precluding NMR study. From the 2D spectra of wild-type GDPMH and the ^{15}N chemical shifts at pH 6.1, only His-124 was largely cationic. The other three histidine residues (His-88, 102, and 142) showed resonance patterns characteristic of neutral NϵH histidines (Figure 6) (*20*, *21*). Since these other residues are less than 20% cationic at pH 6.1, their pK_a values must be significantly lower than 5.5, as confirmed by pH titration (see below).

For His-124, two sets of imidazole ^{15}N and ^1HC resonances, slightly shifted from each other by ≤0.06 ppm, were found, with the downfield set populated 1.4 ± 0.2-fold over the upfield set, suggesting two environments for this catalytic residue in wild-type GDPMH (Figure 6). The proton resonances at 8.50 and 8.53 ppm at pH 6.1 were both absent in the spectrum of the H124Q mutant. Hence, they were both assigned to the HϵC protons of His-124. The chemical shifts of these resonances were followed by 2D $^1H-^{15}N$ HSQC spectra between pH 6.15 and 8.93, yielding nearly identical pK_a values of 7.26 ± 0.12 and 7.25 ± 0.12 for His-124 in the two environments (Figure 7, Table S2, Supporting Information). Above pH 8.93 the HϵC peaks were not observable. The HδC proton peaks of His-124 were observed at 7.32 and 7.28 ppm at pH 6.12 and pH 6.38, at 28 °C but were not visible at higher pH values probably due to exchange broadening.

One-dimensional proton slices of the $^1H-^{15}N$ HSQC spectra of the wild-type enzyme as a function of pH collected between pH 6.15 and 8.82 at 28 °C yielded very similar pK_a values of 7.14 ± 0.06 for the downfield peak and 7.10 ± 0.04 for the upfield peak of His-124 (Table S2, Supporting Information). The Hill coefficients of 0.72−0.79 obtained by fitting the 2D $^1H-^{15}N$ HSQC titrations and their 1D slices may not differ significantly from unity, since forcing the Hill coefficient to be 1.0 did not significantly alter the computed pK_a values within their reported errors (Table S2, Supporting Information). Only the His-124 side chain CϵH and CδH resonances shifted during these titrations, confirming that the pK_a values of the other three histidines were significantly lower than 5.5.

The pK_a value of His-124 determined by 2D $^1H-^{15}N$ HSQC titration, and more rapidly by the 1D slices, was confirmed by the standard 1D proton NMR method (*22*) in 99.9% D_2O at 28 °C. A pH titration of wild-type GDPMH between pH 5.82 and 8.03 monitoring the HϵC resonance of this residue, which did not resolve the two environments of His-124 and which was absent from the spectrum of the H124Q mutant, yielded a pK_a value of 7.23 ± 0.10, with a Hill coefficient (0.95 ± 0.20) indistinguishable from unity (Figure 8) (Table S2, Supporting Information).

The average pK_a of His-124 determined by both 2D and 1D NMR titrations at 28 °C (7.20 ± 0.07) (Table S2) slightly

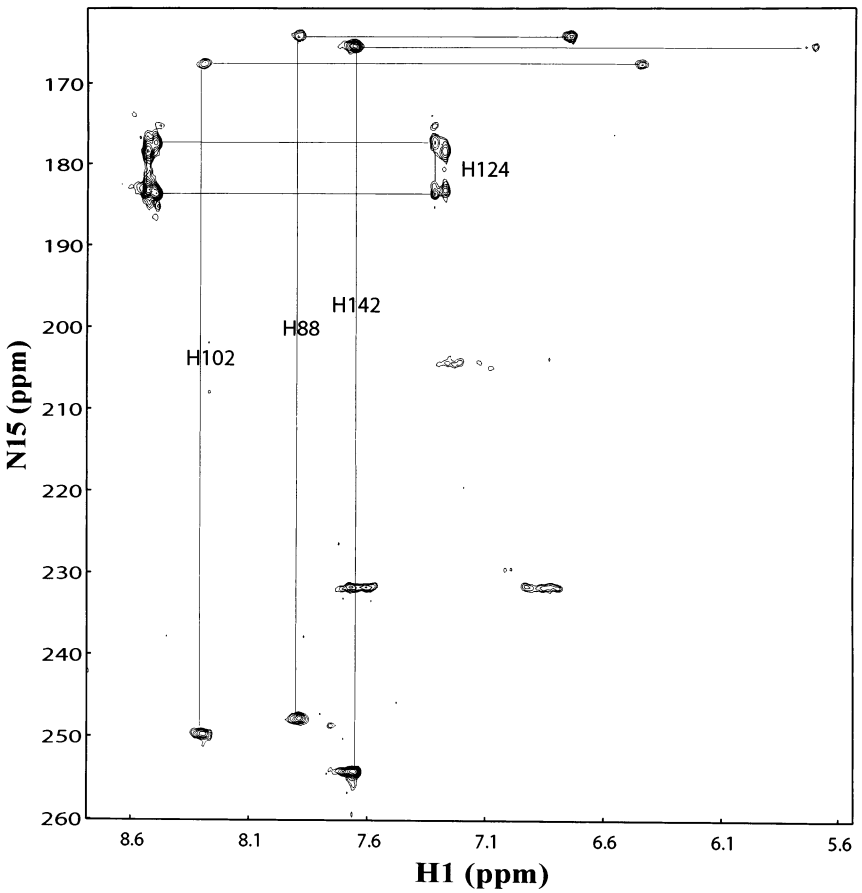

FIGURE 6: Two-dimensional $^1H-^{15}N$ HSQC spectra of the hisitidine region of GDPMH at pH 6.12 and 28 °C showing the protonation states and chemical shift assignments of the four histidine residues of the enzyme, His-88, 102, 124, and 142.

Table 4: Imidazole ^{15}N and ^1HC Chemical Shifts of Histidine Residues at pH 6.1 and 28 °C

	chemical shift (ppm)			
residue	$^{15}N\delta$	$^1H\delta C$	$^{15}N\epsilon$	$^1H\epsilon C$
His-88[a]	247.79	6.74	164.46	7.90
His-102	249.71	6.44	167.55	8.29
His-124	183.24	7.28[b]	177.42	8.53
	183.72	7.32	178.58	8.50
His-142	254.22	5.71	165.55	7.66

[a] From pH 7.0 to 8.1, two sets of resonances were observed, as discussed in the text. [b] The HδC resonance of His-124 was visible only at pH values between 6.1 and 6.4.

exceeds the pK_a determined by the effect of pH on k_{cat}/K_m at the same temperature (6.40 ± 0.20) (Table 2, Figure 2B) by 0.8 ± 0.3 units. This difference in pK_a may have been due to the presence of saturating Mg^{2+} in the kinetic experiments and its absence in the NMR titrations. Glu-70 and other nearby anionic ligands may raise the pK_a of His-124 in the free enzyme and this effect would be neutralized when Mg^{2+} is bound. To test this possibility, we carried out two additional pH titrations monitoring the His-124 HϵC resonance in 1D slices of 2D $^1H-^{15}N$ HSQC experiments. First, titration of wild-type GDPMH between pH 5.60 and 8.54 in the presence of 20 mM $MgCl_2$ yielded a pK_a for His-124 of 6.94 ± 0.04 and a Hill coefficient of 0.94 ± 0.08 (Figure 7A, Table S2). Second, titration of the E70Q mutant in the absence of Mg^{2+}, between pH 6.26 and 8.50, yielded a pK_a for His-124 of 7.01 ± 0.15 and a Hill coefficient of 0.80 ± 0.13. These pK_a values for His-124 were 0.3 ± 0.1 units lower than that found in the Mg^{2+}-free wild-type enzyme at 28 °C and approach the kinetically determined pK_a for k_{cat}/K_m of 6.40 ± 0.20 (Table 2, Figure 2B).

Like His-124, His-88, a residue important to structure and/or catalysis (Table 2), was found by 2D $^1H-^{15}N$ HSQC NMR spectra at pH values 7.0−8.1 to show two sets of imidazole ^{15}N and HC resonances. No significant chemical shift differences were seen in the ^{15}N dimension, but small chemical shift differences of 0.13 and 0.04 ppm were found for HϵC and HδC, respectively. All of these signals disappeared in the spectra of the H88Q mutant. The downfield set of resonances were populated 3.6 ± 0.2-fold over the upfield set, suggesting two environments for this residue. However, the two environments for His-88 were not resolved at other pH values.

Properties of the R52Q and R52K Mutants. While the MutT enzyme requires two divalent cations for activity (*9*) and Ap_4A pyrophosphatase requires three (*10*), GDPMH is the only Nudix enzyme which is known to require only one divalent cation (*8*). Hence, we reasoned that arginine residues in the Nudix box (Figure 1) might function as additional electrostatic catalysts. Arg-52 in GDPMH corresponds to Lys-39 of MutT, which is not conserved in all Nudix enzymes.[6] In MutT, Lys-39 is positioned to neutralize the growing negative charge on the leaving group in the transition state (*6*). In GDPMH the large $10^{2.5}$-fold decrease in the k_{cat} of the R52Q mutant (Table 2) suggests that Arg-52 also acts as an electrostatic catalyst. The k_{cat} was partially rescued in the R52K mutant, in which a much smaller 12-fold decrease in k_{cat} was observed. The partial rescue of k_{cat}

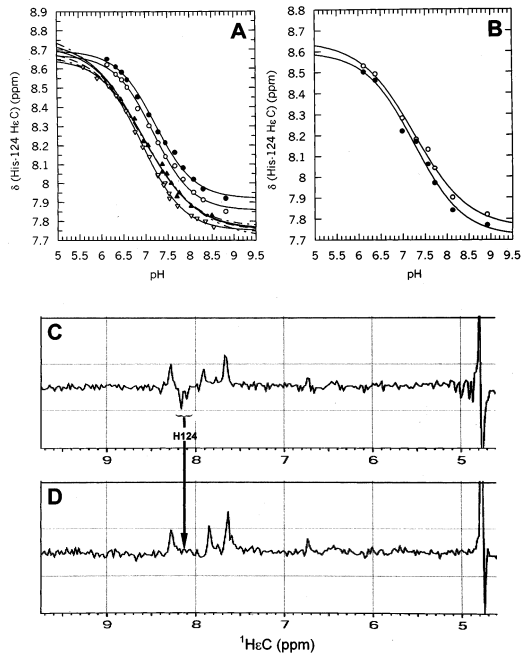

FIGURE 7: pH titrations of His-124 of GDPMH by heteronuclear NMR at 28 °C. (A) pH titration of wild-type GDPMH monitored by 1D slices of the ^{1}H−^{15}N HSQC spectra of histidine side chain resonances in 90% H_2O, 10% D_2O, and 72 mM Na^+ HEPES between pH 6.12 and 8.93. Chemical shift changes of only the HϵC protons of His-124 were observed throughout the course of the titration. Two environments for His-124 were observed with pK_a = 7.26 ± 0.12 (●) and 7.25 ± 0.12 (○) and Hill coefficients = 0.72 ± 0.18 and 0.79 ± 0.21, respectively. Titration of His-124 in the presence of 20 mM $MgCl_2$ (▽) yielded a pK_a = 6.94 ± 0.04 and a Hill coefficient of 0.94 ± 0.08. Titration of His-124 in the E70Q mutant (▲) yielded a pK_a = 7.01 ± 0.15 (−) and a Hill coefficient of 0.80 ± 0.13. Since the E70Q titration curve was incompletely defined, δ1 was varied to estimate the pK_a of the His-124 residue. Data were fit to eq 6 holding the upper limit constant at 8.8 ppm (-·-·-), 8.75 ppm (-··-··), 8.725 ppm (·····), and 8.7 ppm (----). (B) pH Titration of wild-type GDPMH monitored by full 2D ^{1}H−^{15}N HSQC correlation spectra in 90% H_2O and 10% D_2O. The filled circles show the chemical shifts of the downfield HϵC resonance, and the open squares show the chemical shift of the upfield HϵC signal of His-124. (C) One-dimensional slice of the ^{1}H−^{15}N HSQC spectrum of wild-type GDPMH at pH 7.39. Note that the HϵC resonances of His-124 are negatively phased. (D) One-dimensional slice of H124Q at pH 7.46.

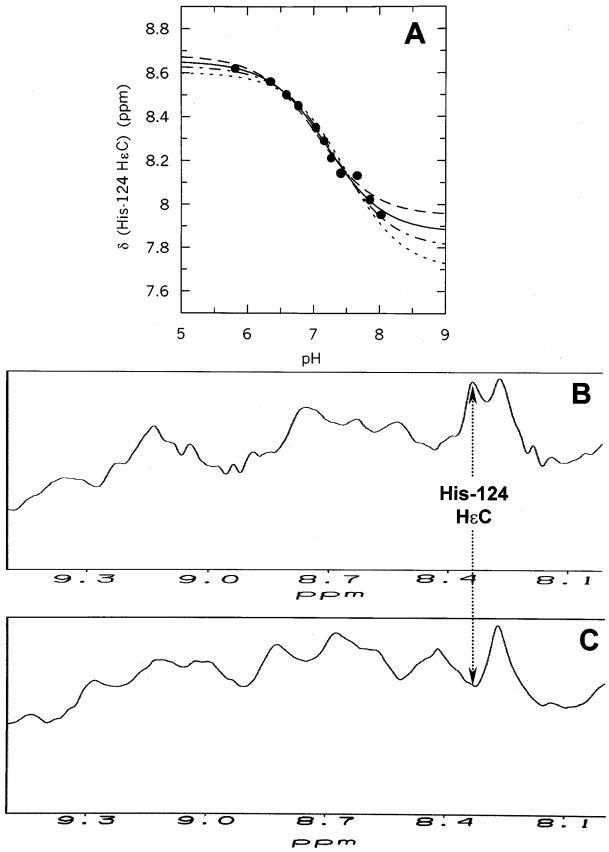

FIGURE 8: pH titration of wild-type GDPMH by one-dimensional ^{1}H NMR in 99.9% D_2O and 72 mM Na^+ HEPES at 28 °C, and assignment of the ^{1}HϵC resonance of His-124. (A) pH titration. Data were fit to eq 6 holding the lower limit of chemical shift constant at 7.8 (-·-·-), 7.7 (·····), or 7.95 ppm (----). (B) One-dimensional spectrum of wild-type GDPMH at pH 7.06 and (C) one-dimensional spectrum of the H124Q mutant of GDPMH at pH 7.09.

by the incorporation of lysine suggests that Arg-52 acts monofunctionally in the transition state. The K_m of the GDP-mannose substrate increased comparably (40-fold) in both the R52Q ($K_m^{GDPmann}$ = 13 ± 3 mM) and R52K ($K_m^{GDPmann}$ = 14 ± 2 mM) mutants, suggesting that Arg-52 acts bifunctionally in the ground state (Table 2).

In a ^{1}H−^{15}N HSQC experiment, the R52Q mutant was titrated with $MgCl_2$ in eight steps in the range of 0.33−20.3 mM $MgCl_2$ (Figure S1, Supporting Information). From the fitted titration curves of four residues which showed significant changes in backbone ^{15}N chemical shifts, the average dissociation constant of Mg^{2+} was 20.7 ± 7.3 mM, approximately 3.5-fold greater than the K_D of Mg^{2+} from the wild-type enzyme (6.0 ± 1.8 mM) (*8*), suggesting some structural perturbation. In the ^{1}H−^{15}N HSQC spectrum, 28 of 171 peaks differed in proton chemical shift by more than 0.05 ppm, and 20 peaks differed in ^{15}N chemical shift by more than 0.5 ppm.

Wild-type GDPMH was previously shown to form an enzyme−M^{2+}−GDP metal bridge complex and to bind GDP with dissociation constant K_3^{GDP} < 0.5 mM in the presence of saturating concentrations of Mg^{2+} (*8*). An HSQC titration of the R52Q mutant with up to 11.5 mM GDP, in the presence of 20.3 mM Mg^{2+}, yielded no change in ^{1}H or ^{15}N chemical shifts. No new resonances were observed during the course of the titration to suggest slow-exchange. Therefore, the dissociation constant of the GDP product, K_3^{GDP}, is estimated to be much greater than 11.5 mM in the R52Q mutant at saturating concentrations of Mg^{2+}, a weakening of GDP binding by at least 23-fold. Hence, Arg-52 interacts strongly with the GDP leaving group.

Properties of the R65Q and R65K Mutants. The Arg-65 residue of GDPMH corresponds to Arg-52 of MutT (Figure 1).[6] In MutT, Arg-52 is thought to position the general base, Glu-53 (*6*). In the absence of a carboxylate general base in GDPMH, a new role for the Arg-65 residue was sought. The R65Q mutant of GDPMH showed a 23.6-fold decrease in k_{cat} and an 81-fold increase in the $K_m^{GDPmann}$ (26 ± 15 mM) (Table 2). Mutation of Arg-65 to lysine resulted in a 12-fold decrease in k_{cat} (0.06 ± 0.01 s^{-1}) and only a 3-fold increase in the $K_m^{GDPmann}$ (1.1 ± 0.2 mM) (Table 2). The rescue of substrate binding by the R65K mutation suggests monofunctional interaction of Arg-65 with substrate in the ground state. The failure of significant rescue of k_{cat} by the

R65K mutant suggests bidentate interaction of Arg-65 in the transition state.

DISCUSSION

The lack of a three-dimensional structure of the Nudix enzyme, GDPMH, limits the elucidation of its catalytic residues to comparisons with other Nudix enzymes of known structure and mechanism such as the MutT enzyme, an NTP pyrophosphohydrolase (*6*, *7*, *11*, *26*). However, GDPMH is an unusual Nudix hydrolase which lacks two conserved Glu residues in its Nudix Box sequence (Figure 1). The absence of a Glu homologous to the general base of MutT (Glu-53) and of a Glu corresponding to a conserved metal ligand, Glu-56 in MutT, makes the GDPMH Nudix box unique. Moreover, GDPMH is the only Nudix enzyme known to catalyze nucleophilic attack at carbon rather than at phosphorus (*5*) and the only one shown to be comparably activated by Mn^{2+} and Mg^{2+} (*8*).

Despite these differences from other well-studied Nudix enzymes, a systematic analysis of the effects of mutations on the catalytic and structural properties of GDPMH has revealed six residues which contribute significantly to catalysis: Glu-70, which serves as a metal ligand; His-124, which likely functions as a general base to deprotonate the attacking water, His-88, and His-102 of unknown function;[7] and Arg-52 and Arg-65, which function as electrostatic catalysts (Tables 2 and 3). The effects of mutating these residues to Gln range from $10^{0.9}$- to $10^{3.4}$-fold decreases in k_{cat} and from 4.4- to 81-fold increases in $K_m^{GDP-mann}$ (Table 2). The product of the effects on k_{cat} of the individual Gln mutants of these six residues ($10^{12.7}$) is comparable to the overall catalytic power of GDPMH of $10^{12.2}$ estimated by comparing k_{cat} of the wild-type enzyme (0.71 s^{-1}) to the pseudo-first-order rate constant ($k = 4.9 \times 10^{-13}$ s^{-1}) for the spontaneous hydrolysis of GDP-mannose (by both C−O and P−O cleavage), extrapolated to 37 °C and pH 9.3 (*27*). Hence, if the effects of these residues on k_{cat} are additive (*28*), then most, if not all, of the catalytic residues may have been identified, providing a quantitative explanation of the mechanism of GDPMH.

Five observations on the E70Q mutant of GDPMH support a metal-coordinating function for Glu-70, which corresponds to an important metal ligand in MutT (Glu-57) (*7*): (i) a $10^{2.2}$-fold decrease in activity of the E70Q mutant (Table 2); (ii) a 3-fold increase in the dissociation constant of Mn^{2+} from the ternary E−Mn^{2+}−GDP complex; (iii) a 20-fold increase in the K_m^{Mg2+} (Table 3); (iv) a decrease in the paramagnetic effect of Mn^{2+} in the E−Mn^{2+}−GDP complex on the relaxation rate of water protons; and (v) large paramagnetic effects of Mn^{2+} in the E−Mn^{2+}−GDP complex on the side chain−NH_2 resonances of Gln-70 in the E70Q mutant (Figure 4, Table S1, Supporting Information), indicating close proximity of bound Mn^{2+} to Gln-70. Similar effects were observed in the E57Q mutant of the MutT enzyme (*7*).

[7] In preliminary $^1H-^{15}N$ HSQC experiments with the GDPMH−Mn^{2+}-GDP complex of the E70Q mutant (to ensure fast Mn^{2+} exchange), paramagnetic effects of bound Mn^{2+} on the volumes of the imidazole resonances of His-124 are 2.5-fold greater than those on His-88, -102, and -142, suggesting that His-124 is closest to the active site Mn^{2+}. Balfour, M. R., and Legler, P. M. (2002) unpublished observations.

The E60Q mutation increased the $K_m^{GDPmann}$ 7.5-fold with little effect on k_{cat} (Table 2), suggesting a modest role for Glu-60 possibly in stabilizing the active site structure. Glu-60 of GDPMH corresponds to Glu-47 of MutT, which is the first residue of helix I and may stabilize this helix (Figure 1) (*11*, *26*).

Unexpectedly, two mutations of GDPMH, E60Q and H142Q, resulted in *decreases* in the K_m^{Mn2+} by factors of 7.0 and 106 respectively, without affecting the K_m^{Mg2+} (Table 3). The selective tightening of Mn^{2+} binding by these mutations may be due to alterations in the tertiary or quaternary structure of the homodimer. The Glu-60 residue is predicted to cap helix I in GDPMH (Figure 1), and removal of Glu-60 may destabilize the helix dipole (*29*). Alternatively, these mutations may relieve negative cooperativity in Mn^{2+} binding in this dimeric enzyme, resulting in higher observed affinities for Mn^{2+}. Negative cooperativity in Mn^{2+} binding by GDPMH was not ruled out in prior metal binding studies (*8*).

In the MutT enzyme, Glu-56 functions as a metal ligand (*6*, *11*), while GDPMH has Ala-69 at this position (Figure 1). By site-directed mutagenesis of GDPMH, Glu-69 was incorporated into this position without significant effects on the kinetically determined affinities of the free enzyme (K_a^{M2+}) or of the enzyme−substrate complex (K_m^{M2+}) for either Mg^{2+} or Mn^{2+} (Table 3). At 37 °C and pH 9.3, a small 3-fold decrease in k_{cat} and a 3.7-fold increase in $K_m^{GDPmann}$ were observed. Hence, in GDPMH, Ala-69 may not be properly positioned to function as a metal ligand.

In our search for the general base, homology considerations revealed only the absence of an appropriately positioned Glu residue. Thus, MutT uses Glu-53, which aligns with Leu-66 in GDPMH (Figure 1),[6] as both a reversible metal ligand and a general base (*6*). In GDPMH, the effect of pH on k_{cat}/K_m revealed a pK_a of 6.38 ± 0.20 and on k_{cat} a pK_a of 6.70 ± 0.06 at 37 °C (Figure 2A). The latter pK_a increased with ionic strength (Figure 5A), consistent with the deprotonation of a cationic His residue in the rate-limiting step, rather than a Glu residue, since the ionization of the carboxyl group would be favored at high ionic strengths, lowering the pK_a. In addition, the measured heat of ionization of the titrating group ($\Delta H^{ionization} = 7.0 \pm 0.67$ kcal/mol) (Figure 5B) was consistent with the deprotonation of a histidine residue and inconsistent with the deprotonation of a Glu (or Asp) residue. The kinetically measured pK_a of 6.70 ± 0.06 for a group influencing k_{cat} thus suggested that a neutral His residue functioned as the general base. GDPMH contains four His residues, His-88, 102, 124, and 142. Gln mutants of each of these His residues led to major decreases in activity in the H88Q and H124Q mutants. The H88Q mutation resulted in a large $10^{2.3}$-fold decrease in k_{cat}, while the H124Q mutant showed the largest decrease in k_{cat}, $10^{3.4}$-fold, and a loss of the pK_a in the relationship of log(k_{cat}) to pH. This pK_a was replaced by a small increase in k_{cat} proportional to $[OH^-]^{0.17}$ at 37 °C (Figure 2D). Since His-124 can be partially replaced by OH^- in the H124Q mutant, His-124 likely functions as the general base in GDPMH.

The pK_a of His-124 was directly measured by three methods, one-dimensional proton NMR in 99.9% D_2O, two-dimensional $^1H-^{15}N$ HSQC spectra of the imidazole side chains, and one-dimensional slices of the $^1H-^{15}N$ HSQC spectra. The last method was found to be superior to the

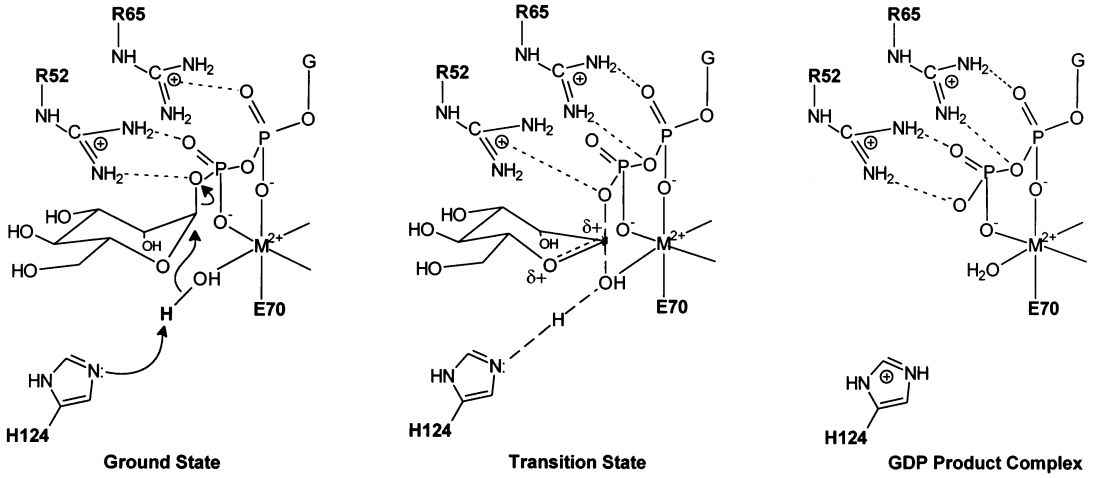

FIGURE 9: Proposed mechanism of the GDPMH reaction. Ground state shows bifunctional hydrogen bonding by Arg-52, monofunctional hydrogen bonding by Arg-65, general base catalysis by His-124, metal coordination by Glu-70, and bidentate metal coordination by the pyrophosphate moiety of GDP-mannose (8). Transition state shows monofunctional hydrogen bonding by Arg-52 and bifunctional hydrogen bonding by Arg-65. GDP product complex shows bifunctional hydrogen binding by both Arg-52 and Arg-65.

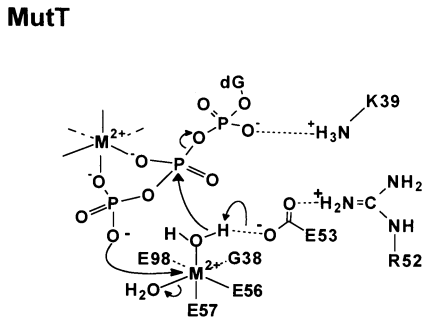

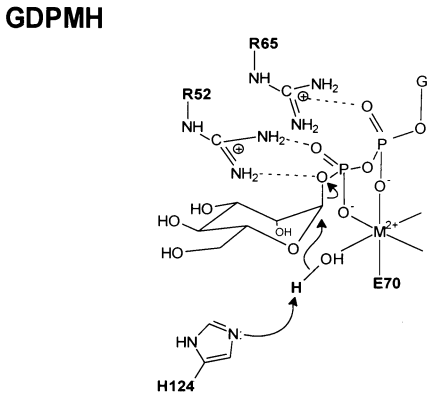

R52	Positions General Base	R65	Important for Substrate Binding
E53	General Base and Reversible Metal Ligand	H124	General Base
E56	Metal Ligand	A69	Not Essential (The A69E mutant had no effect on metal binding)
E47	First residue of Helix I	E60	May stabilize Helix
E57	Metal Ligand	E70	Metal Ligand (probably one of 3 donated by the enzyme)
K39	Neutralizes negative charge in the leaving group in the TS‡	R52	Neutralizes negative charge in the leaving group in the TS‡

FIGURE 10: Comparison of sequence positions and catalytic roles of residues in the mechanisms of the MutT enzyme (left) and of GDPMH (right).

other two in both collection time and resolution (Figures 5, 7, and 8). The differing phases of each resonance facilitated the resolution of partially overlapping signals (Figure 7C,D). In the one-dimensional spectra of the HϵC protons in 99.9% D_2O, significant overlap by partially unexchanged backbone NH protons made identification of the individual histidine HϵC resonances difficult at low pH values and throughout the pH titration. Two-dimensional spectra, although more informative, required at least 2.5 h to collect on a 1.3 mM protein sample. The one-dimensional slices of the 2D HSQC spectra contained easily identifiable HϵC resonances, required ~24 min of collection time for a 0.95 mM protein sample, and did not require deuterium exchange of the backbone NH protons which typically takes 2−3 days to sufficiently remove the overlapping NH resonances. Collection of the $^1H-^{15}N$ HSQC spectra also has the advantage of using 90% H_2O in which the GDPMH enzyme is more stable for up to 3 weeks. All three methods led to comparable pK_a values with an average value of 7.20 ± 0.07 for His-124 (Table S2, Supporting Information). The three other histidines were all found to be neutral NϵH residues at pH 6.1, indicating their pK_a values to be lower than 5.5. Thus, the pK_a of His-124 is closest to the kinetically determined pK_a of 6.40 ± 0.20 obtained from pH versus k_{cat}/K_m at 28 °C and at saturating Mg^{2+} (Table 2, Figure 2B). The 0.8 ± 0.3 unit discrepancy between the NMR and kinetically determined pK_a values of His-124 likely results from the fact that the kinetic data were obtained at saturating Mg^{2+}, which would

neutralize negative charges at the active site, including that of Glu-70, a ligand of the essential Mg^{2+} ion. Consistent with this hypothesis, titration of His-124 in both wild-type GDPMH in the presence of saturating $MgCl_2$ and in the E70Q mutant in the absence of $MgCl_2$ showed significant lowering of the pK_a value of His-124 by 0.3 ± 0.1 units (Figure 7A, Table S2, Supporting Information), approaching the kinetically determined value. The lowering of the pK_a of His-124 in the E70Q mutant also suggests that Glu-70 is in close proximity to the side chain imidazole group of His-124.

Two arginine residues in the Nudix box of GDPMH, Arg-52 and Arg-65, function as electrostatic catalysts. On the basis of the kinetic effects of the R52Q and R65Q mutations and their rescue by the R52K and R65K mutations, we suggest that Arg-52 interacts with the leaving GDP moiety of the GDP-mannose substrate as a bifunctional hydrogen bond donor in the ground state and as a monofunctional donor in the transition state. Arg-65 interacts in an opposite manner, monofunctional in the ground state and bifunctional in the transition state, although other explanations are possible. In Staph nuclease, two arginine residues (Arg-35 and Arg-87), together with enzyme-bound Ca^{2+}, function as electrostatic catalysts. By the same kinetic criteria with mutants used here, supported by X-ray structures, both arginines of Staph nuclease change from monofunctional hydrogen bonding in the ground state to bifunctional hydrogen bonding in the transition state (*15*). It has been suggested that two arginine residues are equivalent to one divalent cation at an enzyme active site (*30*, *31*). Hence, the reason GDPMH and Staph nuclease require only one divalent cation for activity may be due to the presence of two well-placed arginine residues at their respective active sites.

Figure 9 shows a mechanism proposed for GDPMH on the basis of previous kinetic (*5*), stereochemical (*5*), and metal-binding (*8*) studies and the present mutational studies. In the ground state, the GDP moiety of the substrate is held by the divalent cation and by Arg-52 and Arg-65 serving as bifunctional and monofunctional hydrogen bond donors, respectively. His-124 accepts a hydrogen bond from a water ligand of the divalent cation, which is well positioned to attack the C1′ of the sugar, with inversion (*5*). In the transition state, His-124 begins to deprotonate the attacking water, suggested by a 1.8-fold solvent kinetic isotope effect (*5*), the sugar assumes a half-chair conformation possibly with oxocarbenium character (*32*), and Arg-52 and Arg-65 become monofunctional and bifunctional hydrogen bond donors, respectively. In the product complex, the weakly bound sugar has departed, and the tightly bound GDP product is coordinated by the enzyme-bound metal and accepts bifunctional hydrogen bonds from both arginine residues, which explains the potent product inhibition by GDP (*8*).

Figure 10 compares the proposed mechanism of GDPMH with that of the MutT enzyme and also compares in detail the roles of corresponding catalytic residues.[6] Unlike GDPMH, which requires one divalent cation and two arginine residues, MutT requires two divalent cations and Lys-39 as electrostatic catalysts. Arg-52 of MutT, while important to catalysis, does not interact directly with the substrate but may orient the general base, Glu-53. In contrast, the corresponding arginine residue of GDPMH (Arg-65) may interact directly with the substrate.

ACKNOWLEDGMENT

We thank Dr. Ronald Schnaar for helpful advice on carbohydrate chromatography and disaccharide identification protocols and Drs. Maurice Bessman, David Shortle, and Philip A. Cole for valuable suggestions.

SUPPORTING INFORMATION AVAILABLE

One figure (S1) showing a $^1H-^{15}N$ HSQC titration of the R52Q mutant of GDPMH with $MgCl_2$ and two tables: Table S1, summarizing paramagnetic effects of Mn^{2+} on ^{15}N and NH resonances of the E70Q mutant of GDPMH, and Table S2, summarizing the pH titration parameters of His-124 of GDPMH. This information is available free of charge via the Internet at http://pubs.acs.org.

REFERENCES

1. Bessman, M. J., Frick, D. N., and O'Handley, S. F. (1996) *J. Biol. Chem. 271* (41), 25059−25062.
2. Weber, D. J., Bhatnagar, S. K., Bullions, L. C., Bessman, M. J., and Mildvan, A. S. (1992) *J. Biol. Chem. 267*, 16939−16942.
3. O'Handley, S. F., Frick, D. N., Bullions, L. C., Mildvan, A. S., and Bessman, M. J. (1996) *J. Biol. Chem. 271*, 24649−24654.
4. Cartwright, J. L., Britton, P., Minnick, M. F., and McLennan, A. G. (1999) *J. Biol. Chem. 270*, 24086−24091.
5. Legler, P. M., Massiah, M. A., Bessman, M. J., and Mildvan, A. S. (2000) *Biochemistry 39*, 8603−8608.
6. Harris, T. K., Wu, G., Massiah, M. A., and Mildvan, A. S. (2000) *Biochemistry 39*, 1655−1674.
7. Lin, J., Abeygunawardana, C., Frick, D. N., Bessman, M. J., and Mildvan, A. S. (1996) *Biochemistry 35*, 6715−6726.
8. Legler, P. M., Lee, H. C., Peisach, J., and Mildvan, A. S. (2002) *Biochemistry 41*, 4655−4668.
9. Frick, D. N., Weber, D. J., Gillespie, J. R., Bessman, M. J., and Mildvan, A. S. (1994) *J. Biol. Chem. 269*, 1794−1803
10. Conyers, G. B., Wu, G., Bessman, M. J., and Mildvan, A. S. (2000) *Biochemistry 39*, 2347−2354.
11. Lin, J., Abeygunawardana, C., Frick, D. N., Bessman, M. J., and Mildvan, A. S. (1997) *Biochemistry 36*, 1199−1211.
12. Swarbrick, J. D., Bashtannyk, T., Maksel, D., Zhang, X.-R., Blackburn, G. M., Gayler, K. R. and Gooley, P. R. (2000) *J. Mol. Biol. 302*, 1165−1177.
13. Gabelli, S. B., Bianchet, M. A., Bessman, M. J., and Amzel, L. M. (2001) *Nature Struct. Biol. 8*, 467−472.
14. Frick, D. N., Townsend, B. D., and Bessman, M. J. (1995) *J. Biol. Chem. 270*, 24086−24091.
15. Weber, D. J., Gittis, A. G., Mullen, G. P., Abeygunawardana, C., Lattman, E. E., and Mildvan, A. S. (1992) *Proteins: Struct., Funct., Genet. 13*, 275−287.
16. Gill, S. C. and von Hippel, P. H. (1989) *Anal. Biochem. 182*, 319−326.
17. Sarkar, G., and Sommer, S. S. (1990) *BioTechniques 8*, 404−407.
18. Barik, S. (1993) in *PCR Protocol: Current Methods and Applications* (White, B. A., Ed.) Vol. 15, pp 277−286, Humana Press, Inc., Totowa, NJ.
19. Mahuren, J. D., Coburn, S. P., Slominski, A., and Wortsman, J. (2001) *Anal. Biochem. 298*, 241−245.
20. Pelton, J. G., Torchia, D. A., Meadow, N. D., and Roseman, S. (1993) *Protein Sci.* 543−558.
21. Bachovchin, W. W. (1986) *Biochemistry 25*, 7751−7759.
22. Jardetzky, O., and Roberts, G. C. K. (1981) in *NMR in Molecular Biology*, pp 281−284, Academic Press, New York.
23. Flick, J. A., Schnaar, R. L., and Perman, J. A. (1987) *Clin. Chem. 33*, 1211−1212.
24. Dixon, M. (1979) *Enzymes*, 3rd ed., Academic Press, New York, p 163.
25. Cleland, W. W. (1977) *Adv. Enzymol. 45*, 273−387.
26. Abeygunawardana, C., Weber, D. J., Gittis, A, G., Frick, D. N., Lin, J., Miller, A.-F., Bessman, M. J., and Mildvan, A. S. (1995) *Biochemistry 34*, 14997−15005.
27. Cabib, E., and Leloir, L. F. (1954) *J. Biol. Chem. 206*, 779−790
28. Mildvan, A. S., Weber, D. J., and Kuliopulos, A. (1992) *Arch. Biochem. Biophys. 294*, 327−340.

29. Hol, W. G. (1985) *Adv. Biophys. 19*, 133−165.
30. Casareno, R. L. B., Li, D., and Cowan, J. A. (1995) *J. Am. Chem. Soc. 117*, 11011−11012.
31. Mildvan, A. S. (1997) *Proteins, Struct., Funct., Genet. 29*, 401−416.
32. Ly, H. D. and Withers, S. G. (1999) *Annu. Rev. Biochemistry 68*, 487−522.
33. Rost B. and Sander, C. (1993) *J. Mol. Biol. 232*, 584−599.

BI020362E